782. Analysis of the vertical vibration effects on ride comfort of vehicle driver

Aziz Sezgin[1], Yunus Ziya Arslan[2]
Department of Mechanical Engineering, Faculty of Engineering, Istanbul University
Avcilar, Istanbul 34320, Turkey
E-mail: [1]*asezgin@istanbul.edu.tr*, [2]*yzarslan@istanbul.edu.tr*

(Received 20 January 2012; accepted 14 May 2012)

Abstract. Vehicle vibrations affect the health and comfort of the driver and passengers considerably. The aim of this study is to analyze the effects of vertical vehicle vibrations on the driver. To achieve this goal, a human biodynamic model with 11 degrees of freedom was incorporated into a full vehicle model and this combined human-vehicle model was subjected to the road disturbance. After dynamic analysis of the proposed model, root mean square (RMS) acceleration responses of the human body parts over a certain frequency range were obtained. Physiological effects of the vibrations on the human body were analyzed using the criteria specified in International Organization for Standardization (ISO) 2631. Then, in order to observe the effectiveness of a controller on the vibration isolation of human body, sliding mode controller was applied to the model. Comparison of the vibration effects for the uncontrolled and controlled cases of the human-vehicle model was presented. It can be concluded from the results that sliding mode controller considerably reduces whole body vibrations compared with the uncontrolled case and thereby improves the ride comfort satisfactorily.

Keywords: whole body vibration, biodynamic human model, full vehicle model, sliding mode control.

1. Introduction

In everyday life, most people are exposed to vehicle vibrations that affect adversely the health and hence reduce the life quality. Many researchers revealed that those vibrations might cause the loss of performance on working people [1, 2]. Lower acceleration levels of vibrations may cause fatigue failures of different component structures of the spine [3]. Moreover, fractures of spine can also occur with strong excitations [4]. In most of the studies in literature, assessment of the mechanical vibration effects on the human body were performed according to International Standard ISO 2631 and British Standard BS 6841 [5-9].

Ride vibrations of a vehicle during its operation stem from the road roughness and rotating components of the assemblies, driveline and engine. In order to decrease the effect of vehicle vibrations on passengers and drivers, numerous studies have been carried out over years [10, 11]. These studies mostly focused on the optimization of suspension parameters [12, 13], new seat designs [2, 4], and different control strategies [15-19]. Gunston et al. compared the vibration absorption abilities of two different types of seat systems [2]. They concluded that proposed lumped parameter seat model appears best suited to the development of the overall design of a suspension seat and lumped parameter models can assist seat manufacturers in designing new seats, or modifying existing seats. Chen and Huang employed a sliding controller with fuzzy compensation to control a lumped parameter quarter-car active suspension system [20]. They reported that the proposed control scheme significantly suppressed the position oscillation amplitude and acceleration of the sprung mass for improving vehicle ride comfort.

In this study, it was aimed to analyze the disturbing effect of the vehicle ride vibrations on a driver, which is stemmed from road roughness. To achieve this goal, a biodynamic human body model was incorporated into a full vehicle model. Applied road disturbance was the excitation to the combined lumped parameter vehicle-human model and dynamic analysis of this model was carried out. Then, acceleration responses of the seated human body over a frequency range were investigated. Assessment of the acceleration responses of the biodynamic human model was

carried out according to the ISO 2631. Moreover, in order to observe the effectiveness of a controller on the vibration isolation of human body, sliding mode controller (SMC), which is widely used for nonlinear dynamic systems [21-23], was applied to the combined human-vehicle model. Finally, physiological effects of vehicle vibrations on human body for both uncontrolled and controlled situations were evaluated.

2. Vehicle-occupant model

The physical model of the investigated system was formed by a full vehicle model and a human model by considering the human body as a dynamic system as well.

2. 1 Vehicle model

In this study, the human model was incorporated into a non-linear full vehicle model (Fig. 1). The body and wheel masses of the vehicle were assumed to be rigid bodies. The model has seven DOFs which are due to body bounce y, roll s_a, s_y, α, pitch θ and vertical motion of each wheels y_i (i = 1, 2, 3, 4).

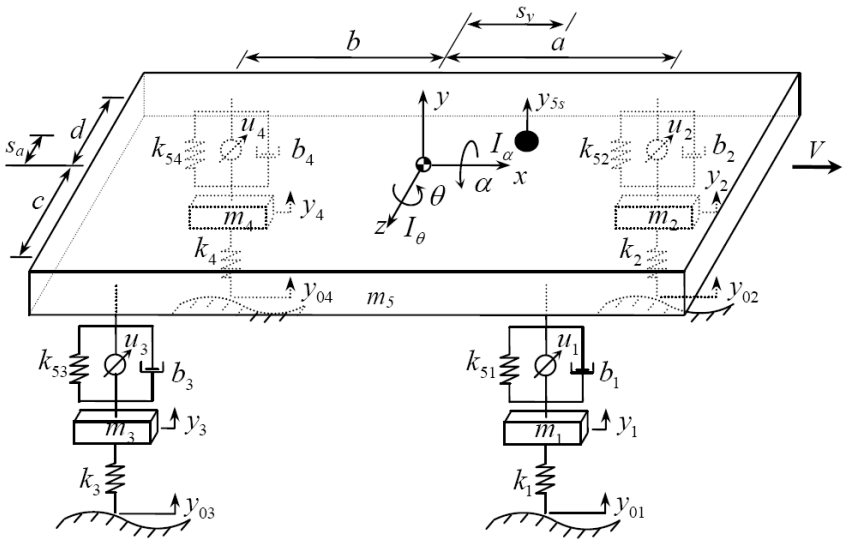

Fig. 1. The full vehicle model

In the model, m_i, m_5, I_α and I_θ stand for the unsprung masses (wheel-axle assembly), sprung mass (vehicle body), and mass moment of inertia for the roll and pitch motions of the vehicle body, respectively. Coefficients of the linear damping and linear springs are b_i, k_i, k_{5i}, respectively and y_{0i} are the road inputs to wheels. V is the velocity of the vehicle in x-direction. Distances of the suspensions to the center of mass of the vehicle body were denoted by a, b, c, d and distances between the center of the gravity and the driver's seat by s_y, s_a. In addition, u_i represents the control force applied to suspensions for the controlled case. Numerical values of the vehicle parameters were given in Appendix A.

2. 2 Human model

A number of lumped parameter models have been introduced for representing the biodynamic characteristics of a human body [3, 24]. In these physical models, human body is

considered as concentrated masses, which represent the different body segments, interconnected by springs and dampers. Since it is simple to analyze and easy to validate with experiments, this type of model has been extensively used in many studies [4]. Liang and Chiang conducted a study to validate the various proposed lumped-parameter human body models by the experimental data from published literature [4].

In this study, in order to carry out a detailed vibration analysis of the human body parts, we used a dynamic model with 11 DOFs and a total mass of 91.7 kg, proposed by Qassem et al. [3] (Fig. 2). All springs and dampers were assumed to be linear.

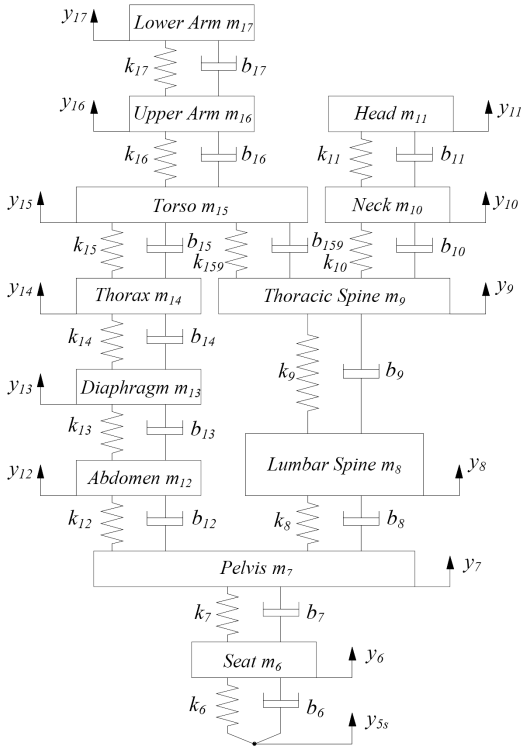

Fig. 2. The biodynamic model of the human body [3]

In the model, human body was segmented into 11 parts. Human back was divided into cervical, thoracic and lumbar spines with same spring and damping coefficients [4]. A seat was also added to the model which transmits the vertical vehicle vibrations to the human body. Biomechanical values of human body parts, namely masses (m_7, m_8, …, m_{17}), springs (k_7, k_8, …, k_{17}) and dampers (b_7, b_8, …, b_{17}), along with the spring and damping coefficients of seat (k_6, b_6), were given in Appendix A.

3. Controller design

Since sliding mode control guarantees system stability and it has a relative simple structure than those based on fuzzy reasoning and neural network [22], we used sliding mode as controller in this study. The sliding mode control approach is recognized as one of the most efficient tools of robust controller design for complex, high-order nonlinear dynamic plants operating under certainty conditions. This method changes the control action with the use of predefined rules during the control process. When the system crosses between stable and unstable trajectories, the

aim of the control is to guide the states to the sliding surface and force them to converge to zero [21]. Therefore, in the controller design process, the sliding surface has to be defined first, and then the control law should be obtained in such a way as to maintain the intended sliding motion.

Equations of motion of the combined vehicle-occupant model were given in state space form, which is a convenient form for controller design, as follows:

$$\dot{\boldsymbol{x}} = \boldsymbol{f}(\boldsymbol{x}) + \boldsymbol{B}\boldsymbol{u} \tag{1}$$

where $\boldsymbol{x} = \left[x_1\ x_2\ x_3 \ldots\ x_{38}\right]^T$ is a $2n \times 1$ state vector and equals to $\left[y_5\ \theta\ \alpha\ y_1\ y_2\ y_3\ y_4\ y_6 \ldots y_{17}\ \dot{y}_5\ \dot{\theta}\ \dot{\alpha}\ \dot{y}_1\ \dot{y}_2\ \dot{y}_3\ \dot{y}_4\ \dot{y}_6 \ldots \dot{y}_{17}\right]^T$. In our case n equals to 19. $\boldsymbol{f}(\boldsymbol{x})$ is the vector of the state equations without control inputs, $\boldsymbol{B}$ is the control force matrix for the controlled case and $\boldsymbol{u} = \left[u_1\ \ u_2\ \ u_3\ \ u_4\right]$ is the vector of the control forces applied to the system (Appendix B).

The sliding surface is defined as:

$$S = \left\{\boldsymbol{x} : \boldsymbol{\sigma}\left(\boldsymbol{x}, t\right) = 0\right\} \tag{2}$$

and the sliding surface can be selected as:

$$\boldsymbol{\sigma} = \boldsymbol{G}\,\boldsymbol{\Delta x} \tag{3}$$

where $\boldsymbol{\Delta x}$ is the difference between the reference value $\boldsymbol{x_r}$ and the system response $\boldsymbol{x}$:

$$\boldsymbol{\Delta x} = \boldsymbol{x_r} - \boldsymbol{x} \tag{4}$$

$\boldsymbol{G}$ includes the sliding surface slopes as:

$$\boldsymbol{G} = \begin{bmatrix} \alpha_1 & 0 & 0 & 0 & 0 & 1 & 0 & 0 & 0 & 0 \\ 0 & \ddots & 0 & 0 & 0 & 0 & \ddots & 0 & 0 & 0 \\ 0 & 0 & \alpha_i & 0 & 0 & 0 & 0 & 1 & 0 & 0 \\ 0 & 0 & 0 & \ddots & 0 & 0 & 0 & 0 & \ddots & 0 \\ 0 & 0 & 0 & 0 & \alpha_n & 0 & 0 & 0 & 0 & 1 \end{bmatrix}_{n \times 2n} \tag{5}$$

For stability analysis, the Lyapunov function candidate $\boldsymbol{v}(\boldsymbol{\sigma})$ has to be positive definite and its derivative has to be negative semi-definite:

$$\boldsymbol{v}(\boldsymbol{\sigma}) = \frac{\boldsymbol{\sigma}^{\mathrm{T}}\boldsymbol{\sigma}}{2} > 0 \tag{6}$$

$$\frac{d\boldsymbol{v}(\sigma)}{dt} = \frac{\dot{\boldsymbol{\sigma}}^{\mathrm{T}}\boldsymbol{\sigma}}{2} + \frac{\boldsymbol{\sigma}^{\mathrm{T}}\dot{\boldsymbol{\sigma}}}{2} \le 0 \tag{7}$$

By using equations (3) and (4):

$$\boldsymbol{\sigma} = \boldsymbol{G}\,\boldsymbol{x}_{\mathrm{r}} - \boldsymbol{G}\,\boldsymbol{x} \tag{8}$$

Equation (8) is separated as follows:

$$\boldsymbol{\sigma} = \boldsymbol{\Phi}(t) - \boldsymbol{\sigma}_{\mathrm{a}}(\boldsymbol{x}) \tag{9}$$

where:

$$\boldsymbol{\Phi}(t) = \boldsymbol{G}\,\boldsymbol{x}_{\mathrm{r}} \tag{10}$$

$$\boldsymbol{\sigma}_{\mathrm{a}}(\boldsymbol{x}) = \boldsymbol{G}\,\boldsymbol{x} \tag{11}$$

Derivation of equation (9) is:

$$\frac{d\boldsymbol{\sigma}}{dt} = \frac{d\boldsymbol{\Phi}(t)}{dt} - \frac{\delta\boldsymbol{\sigma}_{\mathrm{a}}(\boldsymbol{x})}{\delta x}\frac{d\boldsymbol{x}}{dt} \tag{12}$$

This equation has to be equal to zero for the limit case. By using equations (1) and (12):

$$\frac{d\boldsymbol{\Phi}(t)}{dt} - \boldsymbol{G}\left(\boldsymbol{f}(\boldsymbol{x}) + \boldsymbol{B}\boldsymbol{u}_{\mathrm{eq}}\right) = 0 \tag{13}$$

and the equivalent controller force $\boldsymbol{u}_{\mathrm{eq}}$ of the limit case can be found as follows:

$$\boldsymbol{u}_{\mathrm{eq}} = (\boldsymbol{G}\boldsymbol{B})^{-1}\left(\frac{d\boldsymbol{\Phi}(t)}{dt} - \boldsymbol{G}\,\boldsymbol{f}(\boldsymbol{x})\right) \tag{14}$$

The equivalent control is valid only on the sliding surface. Therefore, an additional term should be defined to pull the system to the surface. In order to achieve this, the derivative of the Lyapunov function can be selected as:

$$\dot{\boldsymbol{v}}(\boldsymbol{\sigma}) = -\boldsymbol{\sigma}^{\mathrm{T}}\,\boldsymbol{\Gamma}\,\boldsymbol{\sigma} < 0 \tag{15}$$

here $\boldsymbol{\Gamma}$ is a positive definite matrix:

$$\boldsymbol{\Gamma} = \begin{bmatrix} \Gamma_1 & 0 & 0 & 0 & 0 \\ 0 & \ddots & 0 & 0 & 0 \\ 0 & 0 & \Gamma_i & 0 & 0 \\ 0 & 0 & 0 & \ddots & 0 \\ 0 & 0 & 0 & 0 & \Gamma_n \end{bmatrix}_{n\,x\,n} \tag{16}$$

By using equation (7), along with equations (12) and (15):

$$\boldsymbol{\sigma}^{\mathrm{T}}\dot{\boldsymbol{\sigma}} = -\boldsymbol{\sigma}^{\mathrm{T}}\boldsymbol{\Gamma}\boldsymbol{\sigma} \;\Rightarrow \frac{d\boldsymbol{\sigma}}{dt} + \boldsymbol{\Gamma}\boldsymbol{\sigma} = 0 \tag{17}$$

$$\frac{d\boldsymbol{\sigma}}{dt}+\boldsymbol{\Gamma}\,\boldsymbol{\sigma}=\frac{d\boldsymbol{\Phi}(t)}{dt}-\boldsymbol{G}\left(\boldsymbol{f}(\boldsymbol{x})+\boldsymbol{B}\,\boldsymbol{u}\right)+\boldsymbol{\Gamma}\,\boldsymbol{\sigma}=0 \tag{18}$$

Here, using equation (14), total control input can be written as:

$$\boldsymbol{u}=\boldsymbol{u}_{\text{eq}}+(\boldsymbol{G}\,\boldsymbol{B})^{-1}\boldsymbol{\Gamma}\,\boldsymbol{\sigma} \tag{19}$$

Here $(\boldsymbol{G}\,\boldsymbol{B})^{-1}$ is always equal to mass matrix for mechanical systems. But $\boldsymbol{f}(\boldsymbol{x})$ and $\boldsymbol{B}$ are not well-known. Thus, in this study, it was assumed that equivalent control is the average of the total control. For this assumption, a low-pass filter can be used. This filter can be designed as:

$$\tau\,\dot{\hat{\boldsymbol{u}}}_{\text{eq}}+\hat{\boldsymbol{u}}_{\text{eq}}=\boldsymbol{u} \tag{20}$$

where τ is the time constant of the low pass filter. Finally, the control input can be written as:

$$\boldsymbol{u}=\hat{\boldsymbol{u}}_{\text{eq}}+(\boldsymbol{G}\,\boldsymbol{B})^{-1}\boldsymbol{\Gamma}\,\boldsymbol{\sigma} \tag{21}$$

Elements of the control force vector $\boldsymbol{u}$ were given in Appendix B.

4. Road roughness

In this study, it was assumed that the vibration of the vehicle was only caused by the unevenness of the road surface. There are some indicators of longitudinal unevenness level, which give information about the quality of different road profiles [25]. One of the most important of them is the International Roughness Index (IRI) proposed by Sayers [26]. In this index, road profiles are created by combining the random and harmonic vibrations. Longitudinal road elevation used in this study can be expressed as follows:

$$H(l)=(1-q)\,H_0(l)+q\,H_1(l) \tag{22}$$

where $H_0(l)$ and $H_1(l)$ are the random and harmonic components of the road profile depending on the distance l along the track, respectively, q is a proportion of the random and harmonic components contribution to the road profile. In this study, the vehicle was assumed to travel with a constant velocity of 20 m/s for 5 seconds. Thus, the road roughness was used as disturbance to the vehicle-driver system for a distance of 100 m (Fig. 3). There is a time delay between the front and rear wheel inputs which is equal to $(a+b)/V$. A detailed representation of the calculation of the random and harmonic components of the road profile along with the road parameters, were given in Appendix C.

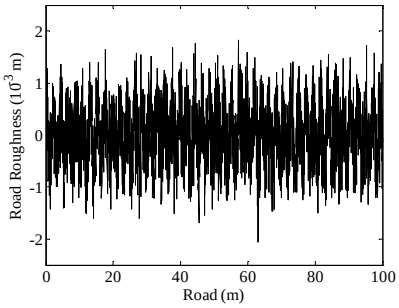

Fig. 3. Profile of the road roughness

5. Vibration exposure criteria

To define the limits of vibration exposure to human body, some vibration criteria were specified in various standards such as ISO 2631 and BS 6841 [7-9]. In our case, evaluation of human exposure to whole body vibration was performed according to ISO 2631 [5]. In this standard, the experimental vibration data collected mainly for sitting and standing postures of human subjects were brought together as a set of vibration criteria curves over the frequency range of 0.1 and 80 Hz [1]. Curves give the vibration level in terms of root mean square (RMS) acceleration, which indicate the general range for onset of the vibration interference and the observed time dependency. Exposure to the vibrations with the frequency ranging between 0.5 Hz to 80 Hz may cause fatigue, discomfort and various health problems, while ranging between 0.1 Hz to 0.5 Hz may result in motion sickness [5]. However, these limits were introduced as recommendations rather than firm boundaries indicating quantitative physiological limits for healthy people [1].

6. Results and discussion

The effects caused by vibration in the human body at any location depend on the vibration frequency [8, 27]. In general, people are considered to be most negatively affected by the vehicle vibrations in the frequency range of 4-10 Hz. The reason behind this phenomenon is that natural frequencies of some of the human body parts coincide with the vehicle vibration frequency which leads to resonance. Kitazaki and Griffin reported that the principal resonance of the human body at about 5 Hz consisted of an entire body mode [28]. Regular exposure to vibration from a vehicle passing through the seat into the driver's body through pelvis can lead to damage and back pain. Amirouche reported that the vibration with the frequency between 1 and 15 Hz becomes harmful, and that resonance effects occur at about 4 to 5 Hz for whole body [29].

RMS acceleration responses of the whole human body model over frequency range were given in Figs. 4a-k. In the figures, for the uncontrolled and controlled cases of the vehicle-occupant model, vibrations transmitted from the vehicle to human body were compared with the vibration interference criteria defined in ISO 2631. According to these criteria, exceeding the exposure specified by the curves results in noticeable fatigue, decreased job proficiency, and different physiological problems [1].

The netural frequencies of the sprung and unsprung masses were 1.2 Hz and 9.5 Hz for the vehicle, respectively. It can be observed from Figs. 4(a-k) that frequency responses of the human body segments show dominant frequencies in the close vicinity of 1.2 Hz and 9.5 Hz. This frequency levels could be related to the sprung and unsprung masses of the vehicle.

In the uncontrolled case, it can be observed from the results that the seat occupant exposed to ride vibrations on a smooth road felt pelvis symptoms up to four hours; head, neck, thoracic spine, abdomen and lumbar spine symptoms between four to six hours; and upper arm, lower arm, torso, thorax and diaphragm symptoms between six to 12 hours. As a result, if it is exposed to ride vibrations around 9 Hz for 6-7 hours, it is possible that a vehicle occupant may feel a general sense of discomfort, lower jaw symptoms, abdominal pains, need to urinate and continuous muscle contraction.

SMC is an important robust control approach for the nonlinear dynamic systems and its one of the major advantage is its stabilizing characteristics for dynamic systems subject to large disturbances [22]. In this study, SMC demonstrated a promising performance in reducing the vibration effects on the human model. In the controlled case, magnitudes of the vibrations on the human body parts are considerably less than those of the uncontrolled case. Unlike in the uncontrolled case, possible head, neck, upper arm, lower arm, torso, thorax, thoracic spine, diaphragm and abdomen symptoms disappeared for the travel duration of $\leq$ 12 hours in the controlled case. In addition, duration of the travel without being exposed to lumbar spine and pelvis symptoms increased to nearly 6 to 12 hours.

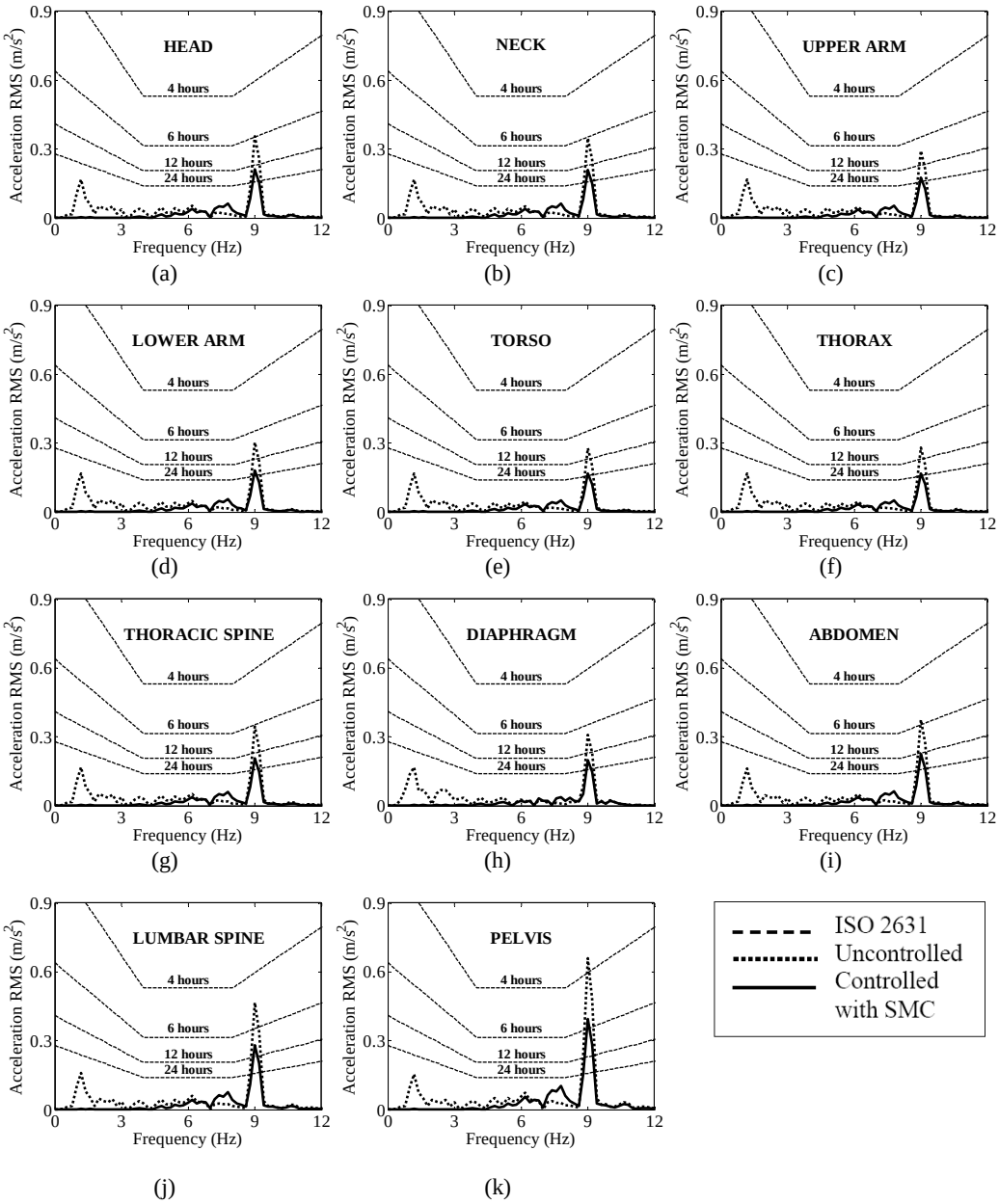

Fig. 4. Comparison of the vibration accelerations of the human body parts, which were obtained for uncontrolled and controlled cases, with that of given in ISO 2631. Comparisons were made for: a) head, b) neck, c) upper arm, d) lower arm, e) torso, f) thorax, g) thoracic spine, h) diaphragm, i) abdomen, j) lumbar spine, k) pelvis

It needs to be remembered that the road profile used in this study belongs to a smooth one and in practice vehicle drivers or passengers may face with much more disturbing road profiles. In addition, it should be noted that only the road roughness was chosen as the excitation, whereas there may be many other discomfort sources, such as rotating components of the engine in vehicles. By taking the other excitation factors along with the road roughness into account, it

can be stated that maximum travel durations within which negative physiological effects are not felt may be less than those recommended in this study.

7. Conclusions

It can be concluded that if it is traveled at a rate of 72 km/h for 5-6 hours on a smooth road in a vehicle with passive suspension system, the driver feels uncomfortable. In the frequency range from 8 to 10 Hz, the seat occupant would feel negative physiological effects such as muscle spasms and abdominal pain. Therefore, a seat occupant should not be exposed to vibrations more than 5 hours under these conditions. However, an active suspension controller, i.e. SMC provided the ability to reduce the vibrations considerably. Vehicle suspension systems with active controller would decrease the negative physiological effects of vehicle vibrations on seat occupants and increase the ride comfort.

Appendix A. System and road parameters

Table A. System and road parameters

m_1	= 66.50 kg	k_1	= 211180 N/m	b_1	= 2015 N·s/m
m_2	= 66.50 kg	k_2	= 211180 N/m	b_2	= 2015 N·s/m
m_3	= 45.18 kg	k_3	= 211180 N/m	b_3	= 935 N·s/m
m_4	= 45.18 kg	k_4	= 211180 N/m	b_4	= 935 N·s/m
m_5	= 1108.64 kg	k_{51}	= 27000 N/m	b_6	= 500 N·s/m
m_6	= 28.00 kg	k_{52}	= 27000 N/m	b_7	= 370.8 N·s/m
m_7	= 27.23 kg	k_{53}	= 20770 N/m	b_8	= 3581.6 N·s/m
m_8	= 2.002 kg	k_{54}	= 20770 N/m	b_9	= 3581.6 N·s/m
m_9	= 4.806 kg	k_6	= 500.0 N/m	b_{10}	= 3581.6 N ·s/m
m_{10}	= 1.08 kg	k_7	= 370.8 N/m	b_{11}	= 3581.6 N·s/m
m_{11}	= 5.445 kg	k_8	= 52621 N/m	b_{12}	= 292.3 N·s/m
m_{12}	= 5.906 kg	k_9	= 52621 N/m	b_{13}	= 292.3 N·s/m
m_{13}	= 0.454 kg	k_{10}	= 52621 N/m	b_{14}	= 292.3 N·s/m
m_{14}	= 1.362 kg	k_{11}	= 52621 N/m	b_{15}	= 292.3 N·s/m
m_{15}	= 32.697 kg	k_{12}	= 877 N/m	b_{16}	= 3581.6 N·s/m
m_{16}	= 5.47 kg	k_{13}	= 877 N/m	b_{17}	= 3581.6 N·s/m
m_{17}	= 5.297 kg	k_{14}	= 877 N/m	b_{159}	= 3581.6 N·s/m
Γ_1	= 500	k_{15}	= 52621 N/m	s_y	= 0.785 m
Γ_2	= 500	k_{159}	= 877 N/m	s_a	= 0.295 m
Γ_3	= 500	k_{16}	= 97542 N/m	a	= 1.945 m
x_{1r}	= 0	k_{17}	= 97542 N/m	b	= 2.115 m
x_{2r}	= 0	L_m	= 2·π /80	c	= 0.58 m
x_{3r}	= 0	C	= 0.9527×10^{-6}	d	= 1.16 m
x_{20r}	= 0	q	= 0.1	α_1	= 0.8
x_{21r}	= 0	L_M	= 2·π/0.1	α_2	= 0.8
x_{22r}	= 0	l_1	= 2.21	α_3	= 0.8
V	= 20 m/s	w	= 2		

Appendix B. Vectors and matrixes

Vector of the state equations without control inputs $\boldsymbol{f}(\boldsymbol{x})$:

$f_1(\boldsymbol{x}) = x_{20}$, $f_2(\boldsymbol{x}) = x_{21}$, $f_3(\boldsymbol{x}) = x_{22}$, $f_4(\boldsymbol{x}) = x_{23}$, $f_5(\boldsymbol{x}) = x_{24}$, $f_6(\boldsymbol{x}) = x_{25}$, $f_7(\boldsymbol{x}) = x_{26}$,

$f_8(\boldsymbol{x}) = x_{27}$, $f_9(\boldsymbol{x}) = x_{28}$, $f_{10}(\boldsymbol{x}) = x_{29}$, $f_{11}(\boldsymbol{x}) = x_{30}$, $f_{12}(\boldsymbol{x}) = x_{31}$, $f_{13}(\boldsymbol{x}) = x_{32}$, $f_{14}(\boldsymbol{x}) = x_{33}$,

$f_{15}(\boldsymbol{x}) = x_{34}$, $f_{16}(\boldsymbol{x}) = x_{35}$, $f_{17}(\boldsymbol{x}) = x_{36}$, $f_{18}(\boldsymbol{x}) = x_{37}$, $f_{19}(\mathbf{x}) = x_{38}$,

$$f_{20}(\boldsymbol{x}) = \frac{1}{m_5}\begin{Bmatrix} -x_8\left(b_1+b_2+b_3+b_4\right)-x_1\left(k_{51}+k_{52}+k_{53}+k_{54}\right)-\cos(x_2)x_9\left[a\left(b_1+b_2\right)-b\left(b_3+b_4\right)\right] \\ -\sin(x_2)\left[a\left(k_{51}+k_{52}\right)-b\left(k_{53}+k_{54}\right)\right]-\cos(x_3)x_{10}\left[d\left(b_2+b_4\right)-c\left(b_1+b_3\right)\right] \\ +\sin(x_3)\left[c\left(k_{51}+k_{53}\right)-d\left(k_{52}+k_{54}\right)\right]+b_1x_{11}+b_2x_{12}+b_3x_{13}+b_4x_{14} \\ +k_{51}x_4+k_{52}x_5+k_{53}x_6+k_{54}x_7 \end{Bmatrix},$$

$$f_{21}(\boldsymbol{x}) = \frac{1}{I_\theta}\begin{Bmatrix} -\cos^2(x_3)x_{10}\left[a^2\left(b_1+b_2\right)+b^2\left(b_3+b_4\right)\right]-\cos(x_2)\sin(x_2)\left[a^2\left(k_{51}+k_{52}\right)+b^2\left(k_{53}+k_{54}\right)\right] \\ -\cos(x_3)x_8\left[a\left(b_1+b_2\right)-b\left(b_3+b_4\right)\right]-\cos(x_2)x_1\left[a\left(k_{51}+k_{52}\right)-b\left(k_{53}+k_{54}\right)\right] \\ -\cos(x_2)\cos(x_3)x_{10}\left[d\left(ab_2-bb_4\right)-c\left(ab_1-bb_3\right)\right] \\ -\cos(x_2)\sin(x_3)\left[d\left(ak_{52}-bk_{54}\right)-c\left(ak_{51}-bk_{53}\right)\right] \\ +\cos(x_2)x_{11}ab_1+\cos(x_2)x_4ak_{51}+\cos(x_2)x_{12}ab_2+\cos(x_2)x_5ak_{52} \\ -\cos(x_2)x_{13}bb_3-\cos(x_2)x_6bk_{53}-\cos(x_2)x_{14}bb_4-\cos(x_2)x_7bk_{54} \end{Bmatrix},$$

$$f_{22}(\boldsymbol{x}) = \frac{1}{I_\alpha}\begin{Bmatrix} -\cos^2(x_3)x_{10}\left[c^2\left(b_1+b_3\right)+d^2\left(b_2+b_4\right)\right]-\cos(x_2)\sin(x_3)\left[c^2\left(k_{51}+k_{53}\right)+d^2\left(k_{52}+k_{54}\right)\right] \\ -\cos(x_3)x_8\left[d\left(b_2+b_4\right)-c\left(b_1+b_3\right)\right]-\cos(x_3)x_1\left[d\left(k_{52}+k_{54}\right)-c\left(k_{51}+k_{53}\right)\right] \\ -\cos(x_2)\cos(x_3)x_9\left[d\left(ab_2-bb_4\right)-c\left(ab_1-bb_3\right)\right] \\ -\cos(x_3)\sin(x_2)\left[d\left(ak_{52}-bk_{54}\right)-c\left(ak_{51}-bk_{53}\right)\right] \\ -\cos(x_3)x_{11}cb_1-\cos(x_3)x_4ck_{51}+\cos(x_3)x_{12}db_2+\cos(x_3)x_5dk_{52} \\ -\cos(x_3)x_{13}cb_3-\cos(x_3)x_6ck_{53}+\cos(x_3)x_{14}db_4+\cos(x_3)x_7dk_{54} \end{Bmatrix},$$

$$f_{23}(\boldsymbol{x}) = \frac{1}{m_1}\begin{Bmatrix} -b_1x_{11}-\left(k_{51}+k_1\right)x_4+b_1x_8+k_{51}x_1+ab_1\cos(x_2)x_9 \\ +ak_{51}\sin(x_2)-cb_1\cos(x_3)x_{10}-ck_{51}\sin(x_3)+k_{51}y_{01} \end{Bmatrix},$$

$$f_{24}(\boldsymbol{x}) = \frac{1}{m_2}\begin{Bmatrix} -b_2x_{12}-\left(k_{52}+k_2\right)x_5+b_2x_8+k_{52}x_1+ab_2\cos(x_2)x_9 \\ +ak_{52}\sin(x_2)+db_2\cos(x_3)x_{10}+dk_{52}\sin(x_3)+k_{52}y_{02} \end{Bmatrix},$$

$$f_{25}(\boldsymbol{x}) = \frac{1}{m_3}\begin{Bmatrix} -b_3x_{13}-\left(k_{53}+k_3\right)x_6+b_3x_8+k_{53}x_1-bb_3\cos(x_2)x_9 \\ -bk_{53}\sin(x_2)-cb_3\cos(x_3)x_{10}-ck_{53}\sin(x_3)+k_{53}y_{03} \end{Bmatrix},$$

$$f_{26}(\boldsymbol{x}) = \frac{1}{m_4}\begin{Bmatrix} -b_4x_{14}-\left(k_{54}+k_4\right)x_7+b_4x_8+k_{54}x_1-bb_4\cos(x_2)x_{10} \\ -bk_{54}\sin(x_2)+db_4\cos(x_3)x_{10}+dk_{54}\sin(x_3)+k_{54}y_{04} \end{Bmatrix},$$

$$f_{27}(\mathbf{x}) = \frac{1}{m_6}\begin{Bmatrix} -k_6\left(x_8-x_7-a\cdot\sin x_2-d\cdot\sin x_3\right)+k_7\left(x_9-x_8\right) \\ -b_6\left(x_{27}-x_{26}-a\cdot x_{21}\cdot\cos x_2-d\cdot x_{22}\cdot\cos x_3\right) \end{Bmatrix},$$

$$f_{28}(\boldsymbol{x}) = \frac{1}{m_7}\begin{Bmatrix} -k_7\left(x_9-x_8\right)+k_8\left(x_{10}-x_9\right)+k_{12}\left(x_{14}-x_9\right) \\ -b_7\left(x_{28}-x_{27}\right)+b_8\left(x_{29}-x_{28}\right)+b_{12}\left(x_{33}-x_{28}\right) \end{Bmatrix},$$

$$f_{29}(\boldsymbol{x}) = \frac{1}{m_8}\left\{-k_8\left(x_{10}-x_9\right)+k_9\left(x_{11}-x_{10}\right)-b_8\left(x_{29}-x_{28}\right)+b_9\left(x_{30}-x_{29}\right)\right\},$$

$$f_{30}(\boldsymbol{x}) = \frac{1}{m_9}\begin{Bmatrix} -k_9\left(x_{11}-x_{10}\right)+k_{10}\left(x_{12}-x_{11}\right)+k_{159}\left(x_{17}-x_{11}\right) \\ -b_9\left(x_{30}-x_{29}\right)+b_{10}\left(x_{31}-x_{30}\right)+b_{159}\left(x_{36}-x_{30}\right) \end{Bmatrix},$$

$$f_{31}(\boldsymbol{x}) = \frac{1}{m_{10}}\left\{-k_{10}\left(x_{12}-x_{11}\right)+k_{11}\left(x_{13}-x_{12}\right)-b_{10}\left(x_{31}-x_{30}\right)+b_{11}\left(x_{32}-x_{31}\right)\right\},$$

$$f_{32}(\boldsymbol{x}) = \frac{1}{m_{11}}\left\{-k_{11}\left(x_{13}-x_{12}\right)-b_{11}\left(x_{32}-x_{31}\right)\right\},$$

$$f_{33}(\boldsymbol{x}) = \frac{1}{m_{12}}\left\{-k_{12}\left(x_{14}-x_{9}\right)+k_{13}\left(x_{15}-x_{14}\right)-b_{12}\left(x_{33}-x_{28}\right)+b_{13}\left(x_{34}-x_{33}\right)\right\},$$

$$f_{34}(\boldsymbol{x}) = \frac{1}{m_{13}}\left\{-k_{13}\left(x_{15}-x_{14}\right)+k_{14}\left(x_{16}-x_{15}\right)-b_{13}\left(x_{34}-x_{33}\right)+b_{14}\left(x_{35}-x_{34}\right)\right\},$$

$$f_{35}(\boldsymbol{x}) = \frac{1}{m_{14}}\left\{-k_{14}\left(x_{16}-x_{14}\right)+k_{15}\left(x_{17}-x_{16}\right)-b_{14}\left(x_{35}-x_{34}\right)+b_{15}\left(x_{36}-x_{35}\right)\right\},$$

$$f_{36}(\boldsymbol{x}) = \frac{1}{m_{15}}\begin{Bmatrix} -k_{15}\left(x_{17}-x_{16}\right)-k_{159}\left(x_{17}-x_{11}\right)+k_{16}\left(x_{18}-x_{17}\right) \\ -b_{15}\left(x_{36}-x_{35}\right)-b_{159}\left(x_{36}-x_{30}\right)+b_{16}\left(x_{37}-x_{36}\right) \end{Bmatrix},$$

$$f_{37}(\boldsymbol{x}) = \frac{1}{m_{16}}\left\{-k_{16}\left(x_{18}-x_{17}\right)+k_{17}\left(x_{19}-x_{18}\right)-b_{16}\left(x_{37}-x_{36}\right)+b_{17}\left(x_{38}-x_{37}\right)\right\},$$

$$f_{38}(\boldsymbol{x}) = \frac{1}{m_{17}}\left\{-k_{17}\left(x_{19}-x_{18}\right)-b_{17}\left(x_{38}-x_{37}\right)\right\}.$$

The control force matrix $\boldsymbol{B}$ for the controlled case:

$$\boldsymbol{B} = \begin{bmatrix} 0 & \ldots & 0 & 0 & \frac{1}{m_5} & \frac{a}{I_\theta} & -\frac{c}{I_\alpha} & -\frac{1}{m_1} & 0 & 0 & 0 & 0 & 0 & \ldots & 0 \\ 0 & \ldots & 0 & 0 & \frac{1}{m_5} & \frac{a}{I_\theta} & \frac{d}{I_\alpha} & 0 & -\frac{1}{m_2} & 0 & 0 & 0 & 0 & \ldots & 0 \\ 0 & \ldots & 0 & 0 & \frac{1}{m_5} & -\frac{b}{I_\theta} & -\frac{c}{I_\alpha} & 0 & 0 & -\frac{1}{m_3} & 0 & 0 & 0 & \ldots & 0 \\ 0 & \ldots & 0 & 0 & \frac{1}{m_5} & -\frac{b}{I_\theta} & \frac{d}{I_\alpha} & 0 & 0 & 0 & -\frac{1}{m_4} & 0 & 0 & \ldots & 0 \end{bmatrix}^T_{4\times 38}$$

Elements of the vector of the control forces applied to the system:

$$u_1 = \frac{bdu_y + du_\theta - (a+b)u_\alpha}{(a+b)(c+d)},$$

$$u_2 = \frac{bcu_y + cu_\theta + (a+b)u_\alpha}{(a+b)(c+d)},$$

$$u_3 = \frac{d(au_y - u_\theta)}{(a+b)(c+d)},$$

$$u_4 = \frac{c\left(au_y - u_\theta\right)}{\left(a+b\right)\left(c+d\right)},$$

$$u_y = \hat{u}_{y(eq)} + m_5 \Gamma_1 \left[\alpha_1 \left(x_{1r} - x_1\right) + \left(x_{20r} - x_{20}\right)\right],$$

$$u_\theta = \hat{u}_{\theta(eq)} + I_\theta \Gamma_2 \left[\alpha_2 \left(x_{2r} - x_2\right) + \left(x_{21r} - x_{21}\right)\right],$$

$$u_\alpha = \hat{u}_{\alpha(eq)} + I_\alpha \Gamma_3 \left[\alpha_3 \left(x_{3r} - x_3\right) + \left(x_{22r} - x_{22}\right)\right],$$

where $\Gamma_1, \Gamma_2, \Gamma_3, \alpha_1, \alpha_2, \alpha_3$ are controller constants which were found by trail. x_{1r}, x_{2r}, x_{3r} are the reference values of the displacements and $x_{20r}, x_{21r}, x_{22r}$ are the reference values of the velocities.

Appendix C. Road roughness

Harmonic component of the road profile is:

$$H_1\left(l\right) = A_d \cdot \cos\left(2\pi l / l_1\right),$$

where A_d is the amplitude of the harmonic undulation, and l_1 is its wavelength:

$$A_d = \sqrt{2D_0 q / (1-q)},$$

here, D_0 is the partial variances of the random component $H_0(l)$ and was expressed as follows:

$$D_0 = C(2\pi)^{-w+1}\left(w-1\right)^{-1}\left({L_M}^{w-1} - {L_m}^{w-1}\right),$$

L_M and L_m are the wavelength range of effectively acting wavelengths of the random road unevenness. C is the unevenness index and w is the waviness. The value of w usually ranges from 1.5 to 3, with the typical value $w = 2$.

References

[1] **Rasmussen G.** Human body vibration exposure and its measurement. Journal of the Acoustical Society of America, Vol. 73, Issue 6, 1983, p. 2229-2229.

[2] **Gunston T. P., Rebelle J., Griffin M. J.** A comparison of two methods of simulating seat suspension dynamic performance. Journal of Sound and Vibration, Vol. 278, Issue 1-2, 2004, p. 117-134.

[3] **Qassem W., Othman M. O., Abdul-Majeed S.** The effects of vertical and horizontal vibrations on the human body. Medical Engineering and Physics, Vol. 16, Issue 2, 1994, p. 151-161.

[4] **Liang C. C., Chiang C. F.** A study on biodynamic models of seated human subjects exposed to vertical vibration. International Journal of Industrial Ergonomics, Vol. 36, Issue 10, 2006, p. 869-890.

[5] International Organization for Standardization ISO 2631-1. Mechanical Vibration and Shock – Evaluation of Human Exposure to Whole – Body Vibration. Part 1: General Requirements. Geneva, 1997.

[6] British Standards Institution BS 6841. Measurement and Evaluation of Human Exposure to Whole – Body Mechanical Vibration. London, 1987.

[7] **Fritz M.** Three-dimensional biomechanical model for simulating the response of the human body to vibration stress. Medical and Biological Engineering and Computing, Vol. 36, Issue 6, 1998, p. 686-692.

[8] **Paddan G. S., Griffin M. J.** Effect of seating on exposures to whole-body-vibration in vehicles. Journal of Sound and Vibration, Vol. 253, Issue 1, 2002, p. 215-241.

[9] **Eger T., Stevenson J., Boileau P.-E, Salmoni A., Vib R. G.** Predictions of health risks associated with the operation of load-haul-dump mining vehicles: Part 1 – Analysis of whole-body vibration exposure using ISO 2631-1 and ISO-2631-5 standards. International Journal of Industrial Ergonomics, Vol. 38, Issue 9-10, 2008, p. 726-738.

[10] **Wikström B.-O., Kjellberg A., Landström U.** Health effects of long-term occupational exposure to whole-body vibration: A review. International Journal of Industrial Ergonomics, Vol. 14, Issue 4, 1994, p. 273-292.

[11] **Hrovat D.** Survey of advanced suspension developments and related optimal control applications. Automatica, Vol. 33, Issue 10, 1997, p. 1781-1817.

[12] **Zhang C. W., Ou J. P., Zhang J. Q.** Parameter optimization and analysis of a vehicle suspension system controlled by magnetorheological fluid dampers. Structural Control and Health Monitoring, Vol. 13, Issue 5, 2006, p. 885-896.

[13] **Tung S. L., Juang Y. T., Lee W. H., Shieh W. Y., Wu W. Y.** Optimization of the exponential stabilization problem in active suspension system using PSO. Expert Systems with Applications, Vol. 38, Issue 11, 2011, p. 14044-1405.

[14] **Mehta C. R., Gite L. P., Pharade S. C., Majumder J., Pandey M. M.** Review of anthropometric considerations for tractor seat design. International Journal of Industrial Ergonomics, Vol. 38, Issues 5-6, 2008, p. 546-554.

[15] **Lee C. M., Bogatchenkov A. H., Goverdovskiy V. N., Shynkarenko Y. V., Temnikov A. I.** Position control of seat suspension with minimum stiffness. Journal of Sound and Vibration, Vol. 292, Issues 1-2, 2006, p. 435-442.

[16] **Taskin Y., Hacioglu Y., Yagiz N.** The use of fuzzy-logic control to improve the ride comfort of vehicles. Strojniski Vestnik - Journal of Mechanical Engineering, Vol. 53, Issue 4, 2007, p. 233-240.

[17] **Poussot-Vassal C., Sename O., Dugard L., Gáspár P., Szabó Z., Bokor J.** A new semi-active suspension control strategy through LPV technique. Control Engineering Practice, Vol. 16, Issue 12, 2008, p. 1519-1534.

[18] **Kim H.-J.** Robust roll motion control of a vehicle using integrated control strategy. Control Engineering Practice, Vol. 19, Issue 8, 2011, p. 820-827.

[19] **Sun W., Li J., Zhao Y., Gao H.** Vibration control for active seat suspension systems via dynamic output feedback with limited frequency characteristic. Mechatronics, Vol. 21, Issue 1, 2011, p. 250-260.

[20] **Chen H. Y., Huang S. J.** A new model-free adaptive sliding controller for active suspension system. International Journal of Systems Science, Vol. 39, Issue 1, 2008, p. 57-69.

[21] **Utkin V. I.** Variable structure systems with sliding modes. IEEE Transactions on Automatic Control, Vol. 22, Issue 2, 1977, p. 212-222.

[22] **Yoshimura T., Kume A., Kurimoto M., Hino J.** Construction of an active suspension system of a quarter car model using the concept of sliding mode control. Journal of Sound and Vibration, Vol. 239, Issue 2, 2001, p. 187-199.

[23] **Yagiz N., Arslan Y. Z., Hacioglu Y.** Sliding mode control of a finger for a prosthetic hand. Journal of Vibration and Control, Vol. 13, Issue 6, 2007, p. 733-749.

[24] **Wan Y., Schimmels J. M.** A simple model that captures the essential dynamics of a seated human exposed to whole body vibration. Advances in Bioengineering, ASME, Vol. BED 31, 1995, p. 333-334.

[25] **Kropac O., Mucka P.** Effects of longitudinal road waviness on vehicle vibration response. Vehicle System Dynamics, Vol. 47, Issue 2, 2009, p. 135-153.

[26] **Sayers M. W.** On the calculation of international roughness index from longitudinal road profile. Transportation Research Record, No. 1501, 1995, p. 1-12.

[27] **Fliegel V., Martonka R., Petrik J.** Measurement and comparison of energy of mechanical vibrations absorbed by humans. Journal of Vibroengineering, Vol. 13, Issue 3, 2011, p. 446-450.

[28] **Kitazaki S., Griffin M. J.** Resonance behaviour of the seated human body and effects of posture. Journal of Biomechanics, Vol. 31, Issue 12, 1998, p. 143-149.

[29] **Amirouche F. M. L.** Biodynamic analysis of the human body subjected to vibration. IEEE Engineering in Medicine and Biology Magazine, Vol. 6, Issue 3, 1987, p. 22-26.